

to be submitted to Nuclear Physics

**SIMPLE PARAMETRIZATION OF THE DENSITY  
EXPANSION AND SKYRME-LIKE FORCES**

**J. TREINER and H. KRIVINE**

Institut de Physique Nucléaire  
Division de Physique Théorique  
91406 ORSAY (France)

September 1978

Laboratoire associé au C. N. R. S.

A SIMPLE PARAMETRIZATION OF THE DENSITY-MATRIX  
EXPANSION AND SKYRME-LIKE FORCES

J. TREINER and H. KRIVINE

Institut de Physique Nucléaire  
Division de Physique Théorique \*  
91406 ORSAY (France)

A SIMPLE PARAMETRIZATION OF THE DENSITY-MATRIX  
EXPANSION AND SKYRME-LIKE FORCES.

J. Treiner, H. Krivine  
I.P.N.

Abstract.

The validity of the density-matrix expansion (DME) is investigated using two different interactions : the Brink and Boecker B1 force and the Campi-Sprung G-0 force. Simple parametrizations of the Hamiltonian density are discussed and the connection between the DME and Skyrme-like forces is examined.

## I - INTRODUCTION

The density matrix expansion (DME) proposed by Negele and Vautherin [1] allows one to construct, from a two-body interaction  $V(\vec{r}_1, \vec{r}_2)$ , an effective nuclear Hamiltonian density, depending on the densities  $\rho_n$  and  $\rho_p$ , their gradients  $\vec{\nabla}\rho_n$ ,  $\vec{\nabla}\rho_p$  and the kinetic energies densities  $\tau_n$  and  $\tau_p$ .

Formally one can separate this Hamiltonian density into two terms : the first one corresponds to the nuclear matter energy at the local densities and the second one, in which the gradients of the densities appear, corrects the departures of the density matrix in the nucleus from its value in nuclear matter. It has been claimed that this second term is essentially determined by the long range behaviour of the force (ref.1, chap.III).

The purpose of the present paper is to further investigate the validity of the DME, and to study its connections with phenomenological forces [2], [3] such as the Skyrme interaction [4] or semi-phenomenological Hamiltonian densities such as those derived within the energy density formalism (EDF) [5].

In section II we compare the results obtained with the DME with those of exact Hartree-Fock (HF) calculations for two different effective forces :

i) that of Brink and Boecker [6] modified by Vautherin and Veneroni [7] hereafter referred to as B18, and ii) the density dependent interaction G-0 of Campi-Sprung [8].

In the framework of the DME, the functional dependence of H in  $V(\vec{r}_1, \vec{r}_2)$  is rather involved and requires the storage of 4 functions of the densities. Since in the H.F. method we essentially need the values of these functions around saturation densities, it is reasonable to look for approximate parametrizations accurate around saturation. For this purpose, we construct in section III a simple expression of the Hamiltonian density H reproducing the results of the exact DME calculations, and we compare it to the functionals obtained with the EDF (section IV).

It is known [9] that the H.F. energy calculated with a Skyrme interaction can be written as the integral of a simple functional (identical in this case to the DME Hamiltonian density, depending linearly on the interaction parameters. In view of the successes of this kind of interaction [10], it is interesting to look for a qualitative and quantitative derivation of these parameters.

Therefore in section V, we construct a Skyrme-type interaction which reproduces accurately the energies per particle, densities, mean square radii and the single particle spectra given by the DME with interaction G=0. We show that a density dependent term proportional to  $\rho^{1/6}$  significantly improves the agreement as compared to a linear density dependence.

## II - DME CALCULATIONS

### 1. Background and notation

In the DME, the angular average of the two-body density matrix  $\rho(\vec{r}_1, \vec{r}_2)$  is expanded around the value  $\bar{R} = \frac{\vec{r}_1 + \vec{r}_2}{2}$  in terms of the relative distance  $\vec{r} = \vec{r}_1 - \vec{r}_2$  :

$$\begin{aligned} \frac{1}{4\pi} \int d\Omega_S \rho(\vec{R} + \frac{\vec{r}}{2}, \vec{R} - \frac{\vec{r}}{2}) &= \frac{1}{4\pi} \int d\Omega_S \sum_m \psi_m^*(\vec{R} + \frac{\vec{r}}{2}) \psi_m(\vec{R} - \frac{\vec{r}}{2}) \\ &= 3 \frac{j_1(rk_F)}{rk_F} \rho(\bar{R}) + 35 \frac{r^2 j_3(rk_F)}{2(rk_F)^3} \left[ \frac{1}{4} \bar{\nabla}^2 \rho(\bar{R}) - \tau(\bar{R}) + \frac{3}{5} \rho(\bar{R}) k_F^2 \right] \\ &\quad + \dots \end{aligned} \quad (1)$$

In formula (1) :

$\rho(\bar{R}) = \sum_m \psi_m(\bar{R})^* \psi_m(\bar{R})$  is the nuclear density, and

$\tau(\bar{R}) = \sum_m \bar{\nabla} \psi_m^*(\bar{R}) \bar{\nabla} \psi_m(\bar{R})$  is the kinetic energy density which

is equal to  $\frac{3}{5} \rho k_F^2$  in nuclear matter with a Fermi momentum  $k_F$  ( $k_F = (3\pi^2 \rho / 2)^{1/3}$ ).

This expansion, truncated at the second term, inserted into the H.F. expression for the potential energy, brings the total energy into the following form :

$$E = \int H(\bar{R}) d^3R, \quad (2)$$

where  $H(\bar{R})$  is the following functional of the densities  $\rho_n(\bar{R})$  and  $\rho_p(\bar{R})$  :

$$H[\rho_n(\bar{R}), \rho_p(\bar{R})] = \rho(\bar{R}) (E/A)_{NM} + \sum_{i=n,p} \left\{ \frac{\hbar^2}{2m_i^*} [\tau(\bar{R}) - \frac{3}{5} \rho(\bar{R}) k_i^2(\bar{R})] + C_i |\bar{\nabla} \rho_i(\bar{R})|^2 \right\} + D \bar{\nabla} \rho_n(\bar{R}) \bar{\nabla} \rho_p(\bar{R}) \quad (3)$$

In equation (3),  $(E/A)_{NM}$  represents the energy per particle in nuclear matter with densities  $\rho_p = \frac{1}{3\pi^2} k_p^3$  and  $\rho_n = \frac{1}{3\pi^2} k_n^3$ . The functional quantities  $C_n \equiv C(\rho_n, \rho_p)$ ,  $C_p \equiv C(\rho_p, \rho_n)$ ,  $D \equiv D(\rho_n, \rho_p)$  and  $\frac{\hbar^2}{2m_i^*}(\rho_n, \rho_p)$  are defined by equations (3.7) to (3.10) and (3.44) of ref.1.

In symmetric nuclear matter ( $\rho_n = \rho_p = \frac{\rho}{2}$ ) with Fermi momentum  $k_F$ , the expression for the effective mass is, for a central force :

$$\frac{\hbar^2}{2m^*} = \frac{\hbar^2}{2m} + B \quad (4)$$

where :

$$B = \frac{35}{\pi k_F} \int_0^\infty \sum_E v^{2S+1, 2T+1}(r) j_1(k_F r) j_3(k_F r) dr \quad (5)$$

and

$$\sum_E V^{2S+1, 2T+1}(r) = V^{11}(r) - 3V^{13}(r) - 3V^{31}(r) + 9V^{33}(r)$$

The labels S and T refer to spin and isospin states.

One should point out that this definition of the effective mass does not coincide with the usual one [11] which is obtained by expanding the nuclear matter one body potential  $U(k)$  in powers of  $k^2$  :

$$\begin{aligned} U(k) &= \sum_{n \leq k_F} \langle kn | V | kn \rangle - \langle kn | V | nk \rangle \\ &= U_0 + k^2 U_2 + \dots \end{aligned} \quad (7)$$

Indeed, this expansion leads to the following effective mass

$$\frac{\hbar^2}{2m^*} = \frac{\hbar^2}{2m} + U_2 \quad (8)$$

$$\text{with } U_2 = \frac{k_F^2}{3\pi} \int_0^\infty \sum_E V^{2S+1, 2T+1}(r) r^3 j_1(k_F r) dr \quad (9)$$

Using the constant value  $U_0$  as potential and the effective mass given by the formula (8) is certainly a good approximation around  $k=0$ . However significant discrepancies appear near the Fermi level  $k_F$  as can be seen on fig.1. On the contrary definitions (4), (5) can be shown to yield a much better overall agreement in the range  $0 \leq k \leq k_F$ . Indeed we prove in appendix A that the effective mass  $B$  of the DME method can be defined as the coefficient of  $k^2$  in a second degree polynomial minimizing the quantity :

$$\begin{aligned} Q(V_n, B) &= \int_0^{k_F} [U(k) - (V_n + B k^2)]^2 P(k) dk \\ \text{where } P(k) &= \frac{3}{k_F^3} k^2 \end{aligned} \quad (10)$$

is the momentum probability density inside the Fermi sea.

## 2. Nuclear matter term

Let us now present the numerical method used in this paper to calculate the function  $(E/A)_{NM}$  appearing in the functional  $H$ .

We first analyze (see Appendix B) the properties of symmetric and asymmetric nuclear matter calculated with various potentials. We then show that it is possible to construct a simple parametrization of  $E/A(k_F, \alpha)$ ,  $\alpha = \frac{\rho_n - \rho_p}{\rho}$ , valid even in the region  $\alpha \sim 1$  (case of neutron gas). For this parametrization which looks like a Taylor expansion around the saturation momentum  $k_{F_0}$  of symmetric nuclear matter, we have adopted the following polynomial form :

$$E/A = k_F^2 (a_0 + a_1 \Delta k + a_2 \Delta k^2 + a_3 \Delta k^3) + \alpha^2 k_F^2 (a_4 + a_5 \Delta k) \quad (11)$$

where

$$\Delta k = k_F - k_{F_0} \quad ,$$

Formula (11) exhibits the expected  $k_F^2$  dependence at low density (kinetic energy term). However the numerical values of the coefficients  $a_i$  have not been determined so as to reproduce exactly this term. Indeed we think that in the DME spirit it is more useful to adjust the values of the coefficients  $a_i$  by requiring an accurate description of nuclear matter properties around  $k_{F_0}$ .

In table (i) we give the numerical values of  $a_i$  for the interactions G-0 and B1 $\beta$  and from fig. (2) and (3) it is seen that they lead to a very good agreement with exact results.

## 3. Functions B, C and D

Figures (4) and (5) show the functions  $C(\rho_n, \rho_p)$ , and  $D(\rho_n, \rho_p)$  with  $\rho_n = \rho_p = \frac{\rho}{2}$ , i.e.  $C(k_F, \alpha=0)$  and  $D(k_F, \alpha=0)$  for various potentials. Since these functions and their derivatives

vary very rapidly at low density, we have preferred to tabulate them on a regular mesh in  $k_F$  and  $a$  rather than in  $\rho_n$  and  $\rho_p$  as is done in reference [16]. The constant step of  $.1 \text{ fm}^{-1}$  in  $k_F$  that we have adopted is for example equivalent to a step in  $\rho$  varying from  $6 \cdot 10^{-5} \text{ fm}^{-3}$  at zero density to  $3.7 \cdot 10^{-2} \text{ fm}^{-3}$  around saturation density. The step in  $a$  was chosen equal to  $.1$ .

The tabulation of  $B$  has been done in the same way and intermediate values needed for the integrals have been obtained with a six points interpolation formula [12]. Our H.F. calculations with the DME functional  $H$  have been performed using the code of Vautherin.

#### 4. Results

Our results are shown in tables (2) and (3) for G-0 and B1 $\beta$  respectively, and a comparison is made with exact\* H.F. calculations [13], [14].

We obtain slightly overbound nuclei (.4 to 1. MeV per particle) and too small radii. In the case of G-0, the radii discrepancy is almost constant (.2 fm) for all nuclei while in the case of B1 $\beta$ , it increases from .1 in  $^{16}\text{O}$  to .3 fm in  $^{90}\text{Zr}$ .

In figs. (6), (7) and (8) we show the effect of the DME approximation on the densities : the DME tends to maintain high densities inside the nuclei and to decrease the surface thicknesses. Except for  $^{208}\text{Pb}$  calculated with G-0 interaction, this produces, in all other cases, a smoothing of the oscillations in comparison to those given by exact H.F. calculations.

Figures (9), (10) and (11) display the spectra of individual levels obtained with G-0 and B1 $\beta$ . The discrepancies with exact HF results are similar for all nuclei : the levels are gene-

---

\*In the case of G-0, center of mass and starting energy corrections have been neglected. In the case of B1 $\beta$ , we included a center of mass correction (direct term only). In both cases, we have used a short range spin-orbit force (see, e.g. ref.1) with strength  $w_0 = -130 \text{ MeV fm}^5$ . We only calculate the direct term of the Coulomb energy.

rally overbound by 1 to 2 MeV near the Fermi surface.

In table (2), fig.(9) and (10) the results of calculations using  $U_2$  for the effective mass (equations (8) and (9)) are also presented and denoted (2). We see that energies per particle, radii, and proton and neutron densities are in good qualitative agreement with those obtained using B (equations (4) and (5)). As could be expected the main differences appear for single particle spectra : since the effective mass calculated with  $U_2$  has a smaller value than that obtained with B (for interaction G-C, .625 instead of .651 at the saturation point of symmetric nuclear matter), it leads to more bound levels and lower level density. This confirms the conclusion of the discussion made in part 1 of the present section : the best results are obtained with the best fit of the Hartree-Fock field  $U(k)$  in the nuclear matter.

### III - PARAMETRISATION OF THE FUNCTIONAL H

We shall now show that we can obtain the previous results in a shorter way by parametrising the 3 matrices  $B(\rho_n, \rho_p)$ ,  $C(\rho_n, \rho_p)$ ,  $D(\rho_n, \rho_p)$ . Since  $B(k_F, \alpha)$  is a smooth function of the variables, we parametrize it with the following simple polynomial formula :

$$B_{\frac{n}{p}} = (b_1 k_F^2 - b_2 k_F^3) (1 + b_3 \alpha) \quad (13)$$

The coefficients  $b_i$  for the interactions G-0 and B1 $\beta$  are given in table (1). With these coefficients, adjusted to give the exact effective mass at the saturation of symmetric nuclear matter, we reproduce accurately the exact functions  $B_n$  and  $B_p$  within the range  $(0, k_{F0})$ .

As mentioned in ref.[1], because of the factor  $r^4$  which appears in the integrals defining C and D, these quantities do not depend on the short distance part of the potential. However, as can be seen on fig.(4) and (5), where the functions C and D calculated

with different potentials are plotted (for  $\alpha = 0$ ), they differ significantly for potentials with the same long distance behaviour (potential of Negele and G-0), showing that C and D also depend on the medium range part of the force. In particular they cannot be reproduced with only the OPEP term which gives zero values of C and D when  $k_F$  is larger than  $1 \text{ fm}^{-1}$ . This value corresponds to the mean density of the surface of the nucleus where the gradients of the densities are large and consequently the contribution to the total energy of the terms involving C and D is important.

So, we cannot hope to determine universal functions C and D valid for any reasonable effective interaction.

From fig. (4) and (5), one sees that a linear function of  $k_F$  provides a reasonable fit of C and D in the region where the gradients of the densities are important ( $.7 < k_F < k_{F_0}$ ). We found that the dependence of D in  $\alpha^2$  is small and could be neglected. We obtained the following expressions :

$$D = d_1 + d_2 k_F \quad (14)$$

From the consideration of fig. (12), one should be tempted on the contrary to consider that a good parametrization of C should take into account its asymmetry dependence. Indeed, one sees that  $C_n (C_p)$  diverges when  $\alpha$  comes close to -1 (+1) as  $(\frac{1}{\rho_n})^{1/3} ((\frac{1}{\rho_p})^{1/3})$ . In an actual nucleus this kind of divergence can only occur at the out most surface. Let us suppose that the neutron density extends further than that of proton (case of  $N > Z$  nuclei), then  $\rho_p$  decreases as  $e^{-2\sqrt{\epsilon_p} \cdot r}$ , where  $\epsilon_p$  is the proton fermi energy. Therefore in spite of the divergence of C, the contribution  $C_p (\bar{v}_p)^2$  to the DME Hamiltonian density vanishes as  $e^{-\frac{10}{3} \sqrt{\epsilon_p} \cdot r}$ . This shows that the exact reproduction of the behaviour of  $C_p$  and  $C_n$  for large values of  $\alpha$  is not really important in actual nuclei.

Near  $\alpha = 0$ , one can write :

$$C_p = C(1 - va)$$

$$C_n = C(1 + va)$$

where  $v$  is a constant.

The terms  $C_n(\bar{\nabla}\rho_n)^2 + C_p(\bar{\nabla}\rho)^2$  of the functional  $H$  then become :

$$C[(\bar{\nabla}\rho_n)^2 + (\bar{\nabla}\rho_p)^2] + vaC[(\bar{\nabla}\rho_n)^2 - (\bar{\nabla}\rho_p)^2] \quad (15)$$

and the second term is always small in the nuclei that we considered (even in  $^{208}\text{Pb}$  as it is the square of the gradients that appears in equation (15)).

For these reasons, we think that the  $\alpha$ -dependence of  $C_n$  and  $C_p$  could be neglected without altering the quality of the DME results and we propose the following linear parametrization :

$$C_n = C_p = C_1 k_F + C_2 \quad (16)$$

The coefficients  $C_1$  and  $C_2$  for G-0 and B1 $\beta$  are given in table (1).

The results obtained with the parametrizations given by eq.(11), (13), (14) and (16) are shown in column (3) of tables (2) and (3). It is seen that proton and neutron radii, energies per particle and single particle spectra of the exact DME calculation (column (1)) are well reproduced. However the agreement is slightly better for G-0 than for B1 $\beta$ .

#### IV - COMPARISON WITH ENERGY DENSITY FORMALISM FUNCTIONALS.

In the preceding section, we have shown that an accurate reproduction of the DME results with G-0 effective interaction could be achieved with a polynomial (in  $k_F$  and  $\alpha$ ) parametrization of the functional quantities  $\frac{E}{A}$ ,  $B$ ,  $C$ ,  $D$ . This parametrization which introduces the 14 coefficients (including the spin-orbite strength) displayed in table (1) gives to the Hamiltonian densities a

form very similar to that derived within the energy density formalism [5]. Using an Hamiltonian density with a structure partly suggested by theoretical considerations, the authors of ref.5 have adjusted the 11 parameters of their functional so as to reproduce masses and charge densities of magic nuclei. In view of the formal similarity of the two Hamiltonian densities, it is interesting to compare the numerical values of our coefficients to those of their corresponding parameters.

We have chosen to compare the parametrization obtained for G-0 interaction to the functional constructed from the set of parameters labelled  $F_2$  in ref.5, which leads to properties of nuclear matter quite similar to those of G-0, as can be seen in table (4). We show in table (8) of appendix B the coefficients  $a_1$  corresponding to the set of parameters  $F_2$  of Beiner and Lombard (B.-L.).

This set of parameters  $F_2$  leads to the following constant values of C and D :

$$\begin{aligned} C &= 51.7 \quad \text{MeV fm}^5 \\ D &= 203.4 \quad \text{MeV fm}^5 \end{aligned}$$

These values cannot be compared directly to those obtained for G-0, which are functions of the density. However, in nuclei where we can assume  $\rho_n = \rho_p = \frac{\rho}{2}$  the gradient terms of the DME functional can be written :

$$C_n (\bar{\nabla} \rho_n)^2 + C_p (\bar{\nabla} \rho_p)^2 + D \bar{\nabla} \rho_n \cdot \bar{\nabla} \rho_p = \frac{1}{4} (2C + D) (\bar{\nabla} \rho)^2 \quad (17)$$

and at the mean density of the surface ( $k_F \approx 1.1 \text{ fm}^{-1}$ ) where the contribution of the terms given in eq.(17) is the most important, we have :

$$2C + D = 280 \text{ MeV fm}^5$$

compared to the value 306.8 in the case of Beiner and Lombard.

Thus, we see that the two functionals are very similar ; the main differences appear essentially in the Fermi

momentum, which is smaller in the case of B.-L., and in the compression modulus which is greater.

This difference in Fermi momenta explains why we obtain smaller radii (1% and 1.6%) in heavy nuclei (respectively  $^{90}\text{Zr}$  and  $^{208}\text{Pb}$ ), with our functional. The single particle spectra and level densities near the Fermi surface are in good qualitative agreement.

#### V - EQUIVALENT SKYRME-TYPE INTERACTION.

We shall now show that it is possible (in the case of interaction G-0) to simplify our parametrization while maintaining the quality of the results and find an Hamiltonian density identical to that obtained with a Skyrme-like interaction. A similar attempt has been done by Negels and Vautherin [15].

The nuclear matter energy of a Skyrme force takes the form :

$$\frac{H}{\rho} = \frac{E}{A} = \frac{3}{5} T_F + \frac{3}{8} t_0 \rho + \frac{t_1}{16} \rho^2 + \frac{3}{80} (3t_1 + 5t_2) \rho k_F^2 \quad (18)$$

where  $T_F$  is the kinetic energy of the Fermi level, and the compression modulus at saturation  $K$  is related to  $\frac{E}{A}$  and  $T_F$  by the relation :

$$K = -15 \frac{E}{A} + \frac{9}{5} T_F + \frac{3t_1}{16} \rho^2 \quad (19)$$

As the  $\rho$ -dependent term of the force is repulsive,  $t_1$  is positive. Then  $K$  is necessarily larger than 300 MeV.

Indeed, in the case of G-0 :

$$\frac{E}{A} = -16.7 \text{ MeV}$$

$$k_F = 1.355 \text{ fm}^{-1}$$

Then :

$$- 15 \frac{E}{A} + \frac{9}{5} T_F = 319 \text{ MeV}$$

so we have :

$$K > 319 \text{ MeV} ,$$

compared to the value 182 MeV of G-0 .

Then it is impossible to find a Skyrme interaction having similar nuclear matter properties as G-0. For this reason we modify the power of the density dependence of the  $t_3$  term and introduce a new parameter  $\beta$ , as in reference [2] and [3].

Equation (18) then becomes :

$$\frac{H}{\rho} = \frac{E}{A} = \frac{3}{5} T_F + \frac{3}{8} t_0 \rho + \frac{t_3}{16} \rho^{1+\beta} + \frac{3}{80} (3t_1 + 5t_2) \rho k_F^2 \quad (20)$$

and the expression for the compression modulus :

$$K = - 15 \frac{E}{A} + \frac{9}{5} T_F + \frac{3t_3}{16} \rho^{1+\beta} \beta [3\beta-2] \quad (21)$$

The symmetry energy is given by :

$$E_S = \frac{1}{3} T_F - \frac{1}{4} t_0 (x_0 + \frac{1}{2}) \rho - \frac{t_3}{16} \rho^{1+\beta} + \frac{1}{6} t_2 \rho k_F^2 \quad (22)$$

and the expression for the effective mass is :

$$\frac{\hbar^2}{2m^*} = \frac{\hbar^2}{2m} + B ,$$

with

$$B = \frac{1}{16} (3t_1 + 5t_2) \rho \quad (23)$$

The functions C and D are constant and given by :

$$C = \frac{3}{32} (t_1 - t_2) \quad (24)$$

$$D = \frac{1}{8} (3t_1 - t_2) \quad (25)$$

$$2C + D = \frac{1}{16} (9t_1 - 5t_2) \quad (26)$$

From equation (21), we see that with  $\beta < \frac{2}{3}$  the compression modulus decreases certainly. So we have considered the two following cases :  $\beta = \frac{1}{6}$  and  $\beta = 1$  (for comparison since it corresponds to the original Skyrme interaction).

It is impossible to determine  $t_1$  and  $t_2$  from equations (23), (24) and (25) simultaneously. But since the combination  $2C+D$  is particularly important when  $\rho_n \sim \rho_p$ , we use equation (26) to determine  $9t_1-5t_2$ . The H.F. results are very sensitive to the choice of the value  $2C+D$ . The best ones are obtained with the coefficients  $C$  and  $D$  determined with the optimization method used in appendix A : we look for the best constant  $\lambda$  which minimizes the quantity :

$$Q(\lambda) = \int_0^{k_{F_0}} [2C(k_F) + D(k_F) - \lambda]^2 P(k_F) dk_F \quad (27)$$

where :

$$P(k_F) = \frac{3}{k_{F_0}^2} k_F^2 ,$$

$C(k_F)$  and  $D(k_F)$  are given by eq. (14) and (16) and  $k_{F_0}$  is the saturation momentum of symmetric nuclear matter. We found  $\lambda = 340.4 \text{ MeV fm}^5$ .

Next, to determine  $3t_1+5t_2$  from equation (23), we minimize the quantity :

$$R(\mu) = \int_0^{k_{F_0}} [B(k_F) - \mu k_F^3]^2 P(k_F) dk_F \quad (28)$$

where  $B(k_F)$  is given by equation (13) with  $\alpha = 0$ .

We found  $\mu = 5.31 \text{ MeV fm}^2$ , which, together with the value of  $\lambda$ , gives  $t_1$  and  $t_2$ . Then the dependence of  $B$  in  $\alpha$  is given by the expression :

$$B_{\frac{\rho}{\beta}} = \frac{1}{4}(t_1+t_2) \rho + \frac{1}{8}(t_2-t_1) \rho_{\frac{\rho}{\beta}}$$

which holds for any Skyrme interaction, and  $C$  and  $D$  are calculated by equations (24) and (25).

Inserting  $t_1$  and  $t_2$  in equations (20) and (22), we determine  $t_0$ ,  $t$ , and  $x_0$  by the saturation properties of G-0 ( $k_{F_0}$ ,  $E_0 = \frac{E}{A}(k_{F_0})$ ,  $E_s$ ). The two sets of parameters obtained are presented in table (5), together with the values of K to which they lead.

One should point out that the choice  $\beta = \frac{1}{6}$  gives a value of  $t_0$  which is twice as large as the usual ones [4]: the mechanism of saturation, not studied here, is certainly very different with this Skyrme-like force from what it is usually.

The results obtained with the two Skyrme-like interactions ( $\beta = \frac{1}{6}$  and  $\beta = 1$ ) are shown in table (6), and compared to those of exact DME calculations.

We see that the linear density dependence ( $\beta=1$ ) of the force gives rise to important discrepancies for energies per particle (.3 to .7 MeV) and for radii (.1 to .2 fm too small). This can be seen also on fig. (13) where we compare the proton density distributions in  $^{16}\text{O}$  and  $^{208}\text{Pb}$ .

On the contrary, the  $\rho^{1/6}$ -dependence of the force gives a good overall agreement with the results of the DME calculations. The same conclusion holds also for the one particle spectra (which are not reproduced here).

## VI - CONCLUSION.

This study shows that the accuracy of the DME approximation is quite sensitive to the initial two body force. Namely, the results of the DME calculations we have performed with G-0 and B1 $\beta$  forces do not confirm those of Negele and Vautherin [1]. With the Negele force the difference between exact H.F. calculations and DME is found to be less than 1.5% for radii, densities and less than 10% for binding energies. However our results confirm those of Sprung et al. [16], radii are found also too small (by 2.5% to 8%) average binding energies too large (by 11% to 18%); they equally confirm

the fact that the differences with the exact H.F. calculations do not depend on the masses of the nuclei.

Moreover our results are better, i.e. closer to those of exact H.F. calculations, with G-0 force than with B1 $\beta$  force. This is explained by Sprung et al. [16] by the very significant differences in the ratio of direct to exchange terms between this two forces, the DME being much better for exchange terms. We can also think that this is correlated to the fact that the B1 $\beta$  force gives densities which are much more oscillating in the central region of the nucleus than the G-0 force where the core is more nuclear matter like. The single-particle energies calculated with the DME reproduce those given by exact H.F. calculations qualitatively. The shift of the levels suggests that the effective masses calculated by the DME are too small.

The simple parametrization of the Hamiltonian we have derived allows us to make the connection between the DME and the EDF approaches [5] where the parameters of the functional H are fitted. Indeed we have seen that our parametrization leads to a good fit to the exact DME results.

In the last part of this work we have attempted to parametrize the Hamiltonian density H by energy functionals derived from Skyrme-like forces. We have shown that this can be achieved in the case of G-0 force provided a  $\rho^{1/6}$ -density dependence is used. Indeed in this case excellent fits to radii, binding energies and single-particle energies have been obtained. For the B1 $\beta$  force we have not been able to reproduce the DME results. This may be due to the lack of density dependence in B1 $\beta$  force.

ACKNOWLEDGMENTS.

We would like to express our appreciation to D. Vautherin for suggesting us this study and constant support during the course of this work. We would also like to express our thanks to H. Flocard for critical reading of the manuscript and illuminating conversations. We also are indebted to X. Campi and C. Schmit for helpful discussions and interesting suggestions. Finally, we are grateful to Pr. D.W.L. Sprung for stimulating comments.

APPENDIX A

The usual definition [11] of the effective mass comes from the expansion of the H.F. field in nuclear matter

$$U(k) = \sum_{n \leq k_F} \langle kn | V | kn \rangle - \langle kn | V | nk \rangle = U_0 + k^2 U_2 + \dots$$

The expansion is truncated to second order and the one particle energy  $\epsilon(k)$  is defined by :

$$\epsilon(k) = \frac{\hbar^2 k^2}{2m} + U(k) = \frac{\hbar^2}{2m} k^2 + U_0 + k^2 U_2 = \frac{\hbar^2}{2m^*} k^2 + U_0$$

where :

$$\frac{\hbar^2}{2m^*} = \frac{\hbar^2}{2m} + U_2 .$$

For a central force, one obtains :

$$U(k) = \frac{2}{\pi} k_F^2 \left\{ \frac{k_F}{3} \int_0^\infty \int_D V(r) r^2 dr - \int_0^\infty r \int_E V(r) j_0(kr) j_1(k_F r) dr \right\} \quad (A1)$$

which gives :

$$U_0 = \frac{2k_F^3}{3\pi} \int_0^\infty \int_D V(r) r^2 dr - \frac{2k_F^2}{\pi} \int_0^\infty \int_E V(r) r j_1(k_F r) dr \quad (A2)$$

$$U_2 = \frac{k_F^2}{3\pi} \int_0^\infty \int_E V(r) r^3 j_1(k_F r) dr \quad (A3)$$

with:

$$\int_D V(r) = \frac{1}{4} (V^{11} + 3 V^{13} + 3 V^{31} + 9 V^{33})$$

$$\int_E V(r) = \frac{1}{4} (V^{11} - 3 V^{13} - 3 V^{31} + 9 V^{33})$$

This formula does not coincide with the expression given by the DME. Indeed, eq.(4.43) of ref.1, which determines the individual wave functions, has the form :

$$[-\bar{\nabla}^2 (\frac{\hbar^2}{2m} + B(n_n, c_p))\bar{\psi} + V_n - E] \phi_n = 0$$

in nuclear matter, where  $\phi_n$  are plane waves,

$$E(k) = (\frac{\hbar^2}{2m} + B) k^2 + V_n$$

The one body potential is then equal to  $V_n + Bk^2$ , which defines the effective mass :

$$\frac{\hbar^2}{2m^*} = \frac{\hbar^2}{2m} + B$$

with :

$$B = \frac{35}{\pi k_F} \int_0^\infty \int_E V(r) j_1(k_F r) j_3(k_F r) dr$$

We will now show that this definition provides a least-square fit of  $U(k)$  by the parabola  $V_n + B k^2$  in the range  $(0, k_F)$  with a weight :

$$P(k) = \frac{4\pi k^2 dk}{\frac{4}{3}\pi k_F^3 dk} = \frac{3k^2}{k_F^3}$$

Indeed, let us consider the quantity :

$$Q(\lambda, \mu) = \int_0^{k_F} \{ U(k) - (\lambda + \mu k^2) \}^2 P(k) dk$$

The following equations :

$$\frac{\partial Q}{\partial \lambda} = 0$$

$$\frac{\partial Q}{\partial \mu} = 0$$

give :

$$\lambda = \langle U(k) \rangle - \mu \langle k^2 \rangle \quad (A4)$$

$$\mu = \frac{\langle k^2 \rangle \langle U(k) \rangle - \langle k^2 U(k) \rangle}{\langle k^2 \rangle^2 - \langle k^4 \rangle} \quad (A5)$$

where :

$$\langle f(k) \rangle = \int_0^{k_F} f(k) P(k) dk$$

Since

$$U(k) = U_D + U_E(k)$$

where  $U_D$  is constant, we obtain :

$$\mu = \frac{\langle k^2 \rangle \langle U_E \rangle - \langle k^2 U_E \rangle}{\langle k^2 \rangle^2 - \langle k^4 \rangle}$$

Equation (A1) then gives :

$$\langle U_E(k) \rangle = -\frac{6k_F}{5\pi} \int_0^\infty \int_E V(r) j_1^2(k_F r) dr$$

and :

$$\langle k^2 U_E(k) \rangle = \frac{6k_F^3}{5\pi} \int_0^\infty \int_E V(r) \left\{ 2j_3(k_F r) - 3j_1(k_F r) \right\} j_1(k_F r) dr$$

Together with the relations :

$$\langle k^2 \rangle = \frac{3}{5} k_F^2$$

$$\langle k^4 \rangle = \frac{3}{7} k_F^4$$

one obtains :

$$\mu = B = \frac{35}{\pi k_F} \int_0^{\infty} \int_E V(r) j_1(k_F r) j_3(k_F r) dr \quad (A6)$$

Inserting this expression in eq. (A4), one has :

$$\lambda = V_n = \frac{2k_F^3}{3\pi} \int_0^{\infty} \int_D V(r) r^2 dr - \frac{3k_F}{\pi} \int_0^{\infty} dr \int_E V(r) j_1(k_F r) \left\{ 2j_1(k_F r) + 7j_3(k_F r) \right\} \quad (A7)$$

Expressions (A6) and (A7) coincide with expressions (A3) and (A2) as  $k_F \rightarrow 0$ .

Indeed :

$$35 j_1(k_F r) j_3(k_F r) \rightarrow \frac{1}{3} j_1(k_F r) (k_F r)^3$$

and :

$$j_1(k_F r) \left\{ 2j_1(k_F r) + 7j_3(k_F r) \right\} = \frac{2k_F r}{3} j_1(k_F r) \left\{ 1 - \frac{(k_F r)^4}{504} + \dots \right\}$$

We show on fig. (1) the H.F. field  $U(k)$  and the two parabolae. It is clear that the DME gives a much better fit in the region where the values of the density are important, and that it leads to a larger value for the effective mass.

## APPENDIX B

The energy of an infinite system of protons and neutrons, with Fermi momenta  $k_p$  and  $k_n$  respectively, can be written (to the first order of perturbation theory) :

$$E = \frac{1}{2} \left\{ \sum_{\substack{m \leq k_p \\ n \leq k_n}} \langle mn | V | mn \rangle + \sum_{m, n \leq k_p} \langle mn | V | mn \rangle + \sum_{m, n \leq k_n} \langle mn | V | mn \rangle + \text{exc. terms} \right\} \quad (B1)$$

The usual quantities of such a system are :

$E_0$  : energy per particle at saturation density.

$k_{F_0}$  : saturation momentum of symmetric nuclear matter.

$E_S = \frac{1}{2} \frac{\partial^2 E/A}{\partial \alpha^2}$  : symmetry energy at the saturation point.

$K = k_{F_0}^2 \frac{\partial^2 E/A}{\partial k_F^2}$  : compression modulus at the saturation point.

The curves  $E/A = f(k_F, \alpha)$  are plotted in fig. (2) and (3) for potentials G-0 and B1 $\beta$  respectively. As already noted by other authors [17], one obtains a decrease of saturation density as  $\alpha$  increases. It can be shown, using an expansion about  $k_{F_0}$ , that the shift  $\Delta k_F$  of the saturation momentum has the form :

$$\frac{\Delta k_F}{k_{F_0}} = - b_1 \alpha^2 - b_2 \alpha^4 \quad (B2)$$

with :

$$b_1 = \frac{k_{F_0}}{K} \left( \frac{\partial E_S}{\partial k_F} \right)_{k_F=k_{F_0}} \quad \text{and} \quad b_2 = \frac{1}{2} \left( \frac{k_{F_0}}{K} \right)^3 \left( \frac{\partial E_S}{\partial k_F} \right)^2 \left( \frac{\partial K}{\partial k_F} - \frac{2K}{k_F} \right)_{k_F=k_{F_0}}$$

We will also need the calculations of  $\frac{\partial E_S}{\partial k_F}$  and  $\frac{\partial K}{\partial k_F}$ .

The results are shown in table (7), where we add, for comparison, the results given with some other effective forces. As can be seen on fig. (14),  $E/A$  has a linear dependence in  $\alpha^2$ , when  $k_F$  is kept constant, up to values of  $\alpha$  near 1. We verified that the coefficient of  $\alpha^4$  in the expansion of  $E/A$  is small (less than .5 for G-0 and B18). Inserting a  $k_F^2$  dependence at low density (to take in account the kinetic energy), one has a parametrization of  $E/A$  of the form :

$$E/A = k_F^2 (a_0 + a_1 \Delta k + a_2 \Delta k^2 + a_3 \Delta k^3) + \alpha^2 k_F^2 (a_4 + a_5 \Delta k)$$

where  $\Delta k = k_F - k_{F_0}$ .

It is easy to see that the  $a_i$  are related to the quantities calculated above by the following relations :

$$a_0 = \frac{E_0}{k_{F_0}^2}$$

$$a_1 = - \frac{2}{k_{F_0}^3} E_0$$

$$a_2 = \frac{K}{2k_{F_0}^4} + 3 \frac{E_0}{k_{F_0}^4}$$

$$a_3 = \frac{1}{k_{F_0}^5} \left[ \frac{k_{F_0}}{6} \frac{\partial K}{\partial k_{F_0}} - 4 E_0 - \frac{4}{3} K \right]$$

$$a_4 = \frac{E_S}{k_{F_0}^2}$$

$$a_5 = \frac{1}{k_{F_0}^2} \left[ \frac{\partial E_S}{\partial k_{F_0}} - 2 \frac{E_S}{k_{F_0}} \right]$$

The results are presented in table (8).

---

\*\* In this work, the coefficient  $a_5$  has been determined to give a good agreement with the function  $E_S(k_F)$  in the range  $0 < k_F < k_{F_0}$ .

The equations (B2) which define the coefficients  $b_1$  and  $b_2$  confirm the inability of usual Skyrme interactions to describe correctly nuclei with large neutron excess. Indeed, in the case of Skyrme forces, the decrease of Fermi momentum when  $\alpha$  increases is practically zero because of the high values of  $K$  and the smallness of  $\frac{\partial E_S}{\partial k}$ .

REFERENCES

- [1] J.W. Negele and D. Vautherin, Phys. Rev. C5 (1972) 1472 ; C11 (1975)
- [2] S.A. Moszkowski, Phys. Rev. C2 (1970) 402 ;  
J.V. Eubers and S.A. Moszkowski, Phys. Rev. C6 (1972) 217
- [3] H.S. Köhler, Nucl. Phys. A162 (1971) 385 ; A170 (1971) 88
- [4] M. Beiner, H. Flocard, Nguyen Van Giai and P. Quentin, Nucl. Phys. A238 (1975) 29
- [5] M. Beiner and R.J. Lombard, Ann. of Phys., Vol.86, n°2 (1974), 262
- [6] D.M. Brink and E. Boecker, Nucl. Phys. A91 (1967) 1
- [7] M. Veneroni and D. Vautherin, Phys. Lett. 29B (1969) 203
- [8] X. Campi and D.W. Sprung, Nucl. Phys. A194 (1972) 401
- [9] D. Vautherin and D.M. Brink, Phys. Rev. C5 (1972) 626
- [10] H. Flocard, P. Quentin, D. Vautherin, M. Veneroni and A.K. Kerman, Nucl. Phys. A231 (1974) 176
- [11] G.E. Brown, "Theory of nuclear models and forces", North-Holland Publishing Company, Amsterdam 1967
- [12] M. Abramowitz and I.A. Stegun, "Handbook of Mathematical functions", Nat. Bureau of Standards, Washington 1964, p.883
- [13] D. Vautherin, Thèse, Orsay 1969, unpublished
- [14] X. Campi, private communication
- [15] J.W. Negele and D. Vautherin, Phys. Rev. C11 (1975) 1031
- [16] D.W.L. Sprung, M. Vallieres, X. Campi and Che-Ming Ko, Preprint Mc Master University 1975
- [17] A.G.W. Cameron and R.A. Weiss (Canadian Journ. of Phys. 47, (1969) 2171)
- [18] J.L. Lvinger and L.M. Simmons, Phys. Rev. 124 (1961) 916

- 1191 G. Saunier and J.M. Pearson, Phys. Rev. C1 (1970) 1353
- 1201 C.W. Nestor, K.T.R. Davies, S.J. Krieger and M. Baranger, Nucl. Phys. A113 (1968) 14.

TABLE CAPTIONS

- Table 1. Values of the coefficients used in the parametrization of the DME functional for interaction G-0 and  $B_{1\beta}$  (eq.11,13, 14,16).
- Table 2. Binding energy per nucleon (in MeV), proton and neutron radii (in fm) calculated with G-0 force (see footnote page 6),  
 column (0) refers to exact H.F. calculations  
 column (1) refers to exact DME calculations  
 column (2) refers to exact DME calculations, except for the effective mass, calculated using  $U_2$  eq.(9) instead of B eq.(5).  
 column (3) refers to calculations done with the parametrization of the functional obtained by the DME.
- Table 3. Binding energy (in MeV), proton and neutron radii (in fm) calculated with  $B_{1\beta}$  force (see footnote page 6). The labels (1) and (3) have the same meaning as in table 2.  
 $m^*$  is the effective mass calculated with eq.(8) and (9).
- Table 4. Comparison of nuclear matter properties calculated with G-0 and with one of the functionals used by Beiner and Lombard [5].
- Table 5. Parameters of Skyrme-forces : SG-0 refer to the Skyrme-type forces constructed starting from G-0. We give for comparison the parameters of the Skyrme force SKY 3 of ref.[4]  $t_0$  in MeV.fm<sup>3</sup>,  $t_1$  in MeV.fm<sup>5</sup>,  $t_2$  in MeV.fm<sup>5</sup>,  $t_3$  in MeV.fm<sup>6</sup>.
- Table 6. Comparison of the results of DME calculations (column (1)) with the results obtained from the two Skyrme-type forces constructed : with a  $\rho^{1/6}$  dependence (column (4)) and with a  $\rho$ -dependence (column (5)).

Table 7. Nuclear matter properties of various forces. All the quantities are in MeV except  $\frac{\partial E_S}{\partial k}$  in MeV.fm.

Table 8. Coefficients of the parametrization of E/A in nuclear matter as a function of  $k_F$  and  $\alpha$ .  $b_1$  and  $b_2$  give the shift of the saturation momentum when  $\alpha$  increases (eq.(B2)).

Table 1.

	$a_0$	$a_1$	$a_2$	$a_3$	$a_4$	$a_5$	$b_1$	$b_2$	$b_3$	$c_1$	$c_2$	$d_1$	$d_2$
G-0	-9.1	13.43	12.13	-7.9	-19.33	3.3	8.33	-1.6	.47	-66.	111.	643.	-384.
B1B	-7.44	10.27	10.19	-5.3	23.69	14.	20.47	-3.68	.17	-136.	205.	692.	-342.6

Table 2.

	$^{16}\text{O}$				$^{40}\text{Ca}$			
	0	1	2	3	0	1	2	3
E/A	-6.21	-6.90	-6.94	-6.89	-7.29	-8.22	-8.26	-8.21
$r_n$	2.81	2.68	2.66	2.69	3.52	3.34	3.33	3.34
$r_p$	2.83	2.72	2.68	2.72	3.57	3.40	3.39	3.40

	$^{48}\text{Ca}$				$^{90}\text{Zr}$			
	0	1	2	3	0	1	2	3
E/A	-7.42	-8.47	-8.50	-8.45	-7.78	-8.71	-8.73	-8.69
$r_n$	3.78	3.57	3.55	3.57	4.44	4.23	4.23	4.23
$r_p$	3.58	3.38	3.37	3.39	4.35	4.15	4.16	4.15

	$^{208}\text{Pb}$			
	0	1	2	3
E/A	-7.24	-8.05	-8.07	-8.03
$r_n$	5.71	5.57	5.58	5.57
$r_p$	5.50	5.34	5.37	5.35

Table 3.

		<sup>16</sup> O		
		0	1	3
E/A		-6.05	-6.41	-5.95
r <sub>n</sub>		2.65	2.56	2.58
r <sub>p</sub>		2.67	2.60	2.62

		<sup>40</sup> Ca		
		0	1	3
E/A		-6.43	-7.21	-6.89
r <sub>n</sub>		3.38	3.20	3.20
r <sub>p</sub>		3.43	3.26	3.26

		<sup>48</sup> Ca		
		0	1	3
E/A		-6.10	-7.21	-6.88
r <sub>n</sub>		3.76	3.46	3.48
r <sub>p</sub>		3.51	3.22	3.23

		<sup>90</sup> Zr		
		0	1	3
E/A		-6.28	-7.13	-7.06
r <sub>n</sub>		4.37	4.06	4.07
r <sub>p</sub>		4.25	3.94	3.94

Table 4.

	F2	G-0
E <sub>O</sub>	-16	-16.7
k <sub>F</sub>	1.32	1.36
K	280	182
E <sub>S</sub>	34	35.5
$\frac{m^{3/2}}{m}$	.67	.625

Table 5.

	$\beta$	t <sub>0</sub>	t <sub>1</sub>	t <sub>2</sub>	t <sub>3</sub>	x <sub>G</sub>	K
SG-0	1/6	-2248	558.8	-23.7	11224 <sup>**</sup>	.715	253
	1	-1089	558.8	-83.7	8272	.412	363
SKY3	1	-1129	395	-95	14000	.450	356

(\*\*) in MeV.fm<sup>3/2</sup>.

Table 6.

	$^{16}\text{O}$			$^{40}\text{Ca}$			$^{60}\text{Ca}$		
	1	4	5	1	4	5	1	4	5
E/A	-6.90	-7.04	-6.20	-8.22	-8.22	-7.35	-8.47	-8.39	-7.80
$r_n$	2.68	2.67	2.62	3.34	3.34	3.29	3.57	3.58	3.52
$r_p$	2.72	2.70	2.64	3.40	3.39	3.33	3.38	3.41	3.30

	$^{90}\text{Zr}$			$^{208}\text{Pb}$		
	1	4	5	1	4	5
E/A	-8.71	-8.63	-8.11	-8.05	-7.86	-7.41
$r_n$	4.23	4.23	4.17	5.57	5.54	5.43
$r_p$	4.15	4.16	4.05	5.34	5.36	5.14

Table 7.

Pot.	$k_{F_0}$	$E_0$	$E_S$	K	$\frac{\partial K}{\partial k}$	$\frac{\partial E_S}{\partial k}$
LEV [18]	1.39	-17.35	32	270	1360	68.5
PEAR [19]	1.35	-15.3	31	240	1205	24.
BAR [20]	1.38	-14.9	42.4	293	1518	106.
$B_1B$	1.45	-15.65	49.8	184	616	98.1
G-0	1.36	-16.7	35.5 <sup>**</sup>	182	619	58.3
SG-0	1.36	-16.7	35.5	253	1220	29.5
SKY3	1.29	-15.9	28.2	356	2422	7.9

\* With the rearrangement symmetry energy.

Table 8.

Pot.	$a_0$	$a_1$	$a_2$	$a_3$	$a_4$	$a_5$	$b_1$	$b_2$
$B_1\beta$	-7.44	10.27	10.19	- 5.3	23.69	14.0	.77	.85
G-0	-9.1	13.43	12.13	- 7.9	19.33	3.30	.36	.17
SG-0	-9.1	13.43	22.70	2.0	19.33	1.05	.16	.06
SKY3	-9.5	14.79	47.1	30.6	16.92	-8.2	.03	.003
B.-L.	-9.2	13.89	30.3	9.7	19.51	4.47	-	-

## FIGURE CAPTIONS

- Fig.1. One body H.F. potential  $U(k)$  calculated with G-0 force labelled (0). Label (2) refers to the expansion of  $U(k)$  around  $k=0$  up to second order. Label (1) refers to the DME expansion.
- Fig.2. Energy per particle (in MeV) in nuclear matter as a function of  $k_F$  and  $a$  calculated with G-0.
- Fig.3. Energy per particle (in MeV) in nuclear matter as a function of  $k_F$  and  $a$  calculated with B18.
- Fig.4. Function  $C(k_F, 0)$  is plotted for various potentials : OPEP only, Negele interaction, Campi-Sprung interaction G-0, and SKY referring to SKY3 in ref.[4].
- Fig.5. Function  $D(k_F, 0)$  is plotted for the same interaction as fig.4.
- Fig.6. Proton density distributions calculated with G-0. The exact H.F. calculation is labelled (0), the DME calculation (1).
- Fig.7. Neutron and proton density distributions calculated with G-0. The exact H.F. calculation is labelled (0), the DME calculation (1) and the DME calculation with an effective mass defined by eq.(4) and (5) is labelled (2).
- Fig.8. Neutron and proton density distributions calculated with B18 using exact H.F. calculations (Label (0)) and DME method (label (1)).
- Fig.9. Single particle spectra in the case of G-0. The exact H.F. and calculation is labelled (0), the DME calculation (1) and the
- Fig.10 DME calculation with an effective mass defined by eq.(4) and (5) is labelled (2).

Fig.11. Single particle spectra in the case of B18. The exact H.F. calculation is labelled (0), the DME calculation (1).

Fig.12. Plot of  $C_n$  and  $C_p$  (in  $\text{MeV}\cdot\text{fm}^5$ ) as a function of  $a$  for various values of  $k_F$ .

Fig.13. Proton density distributions in  $^{16}\text{O}$  and  $^{208}\text{Pb}$  (in  $\text{fm}^{-3}$ ). We compare the results of the DME (label (1)) with those obtained with the two Skyrme-type forces : with a  $\rho^{1/6}$  dependence (label (4)) and with a  $\rho$ -dependence (label (5)).

Fig.14. Energy per particle (in MeV) in nuclear matter calculated with G-0 as a function of  $a^2$  for various values of  $k_F$ .

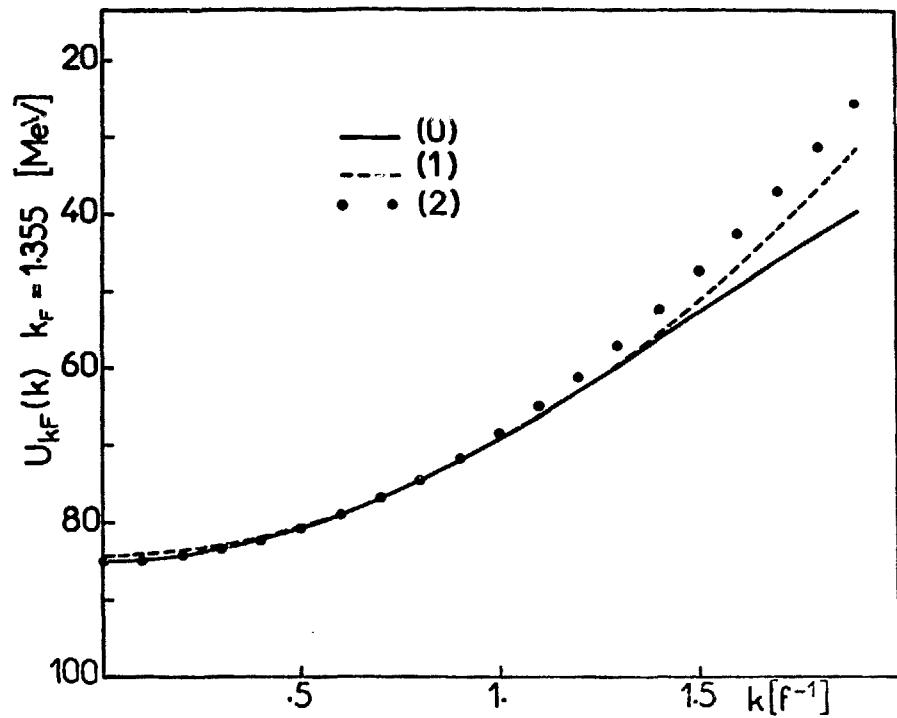


Fig. 1.

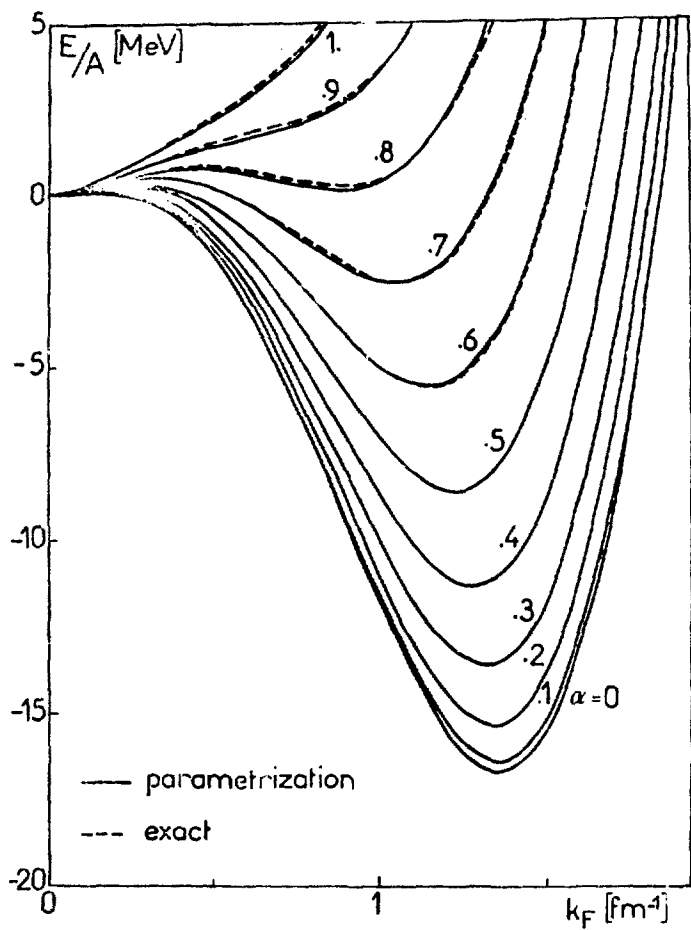


Fig. 2.

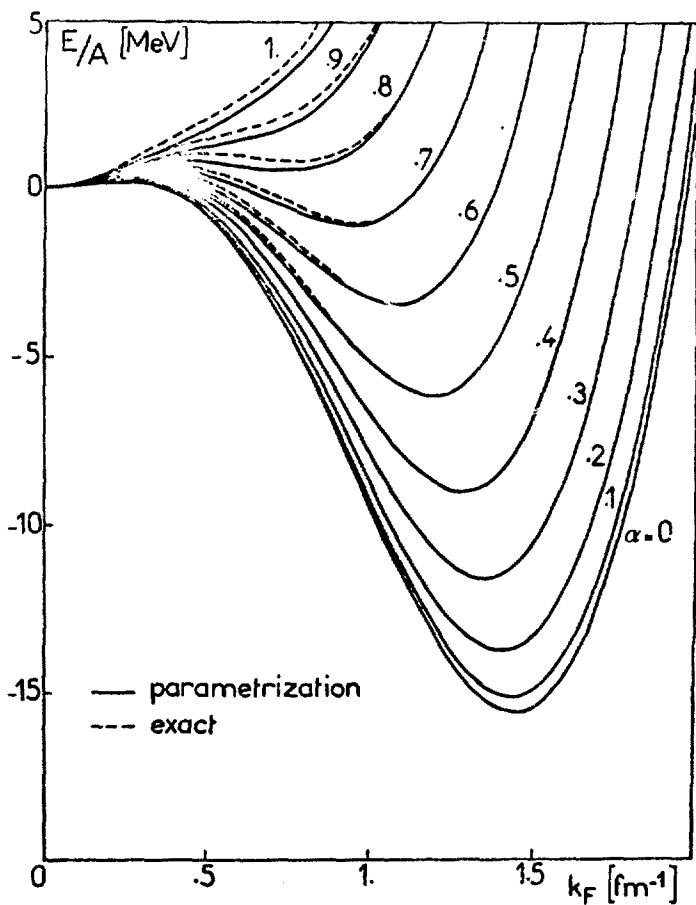


Fig. 3.

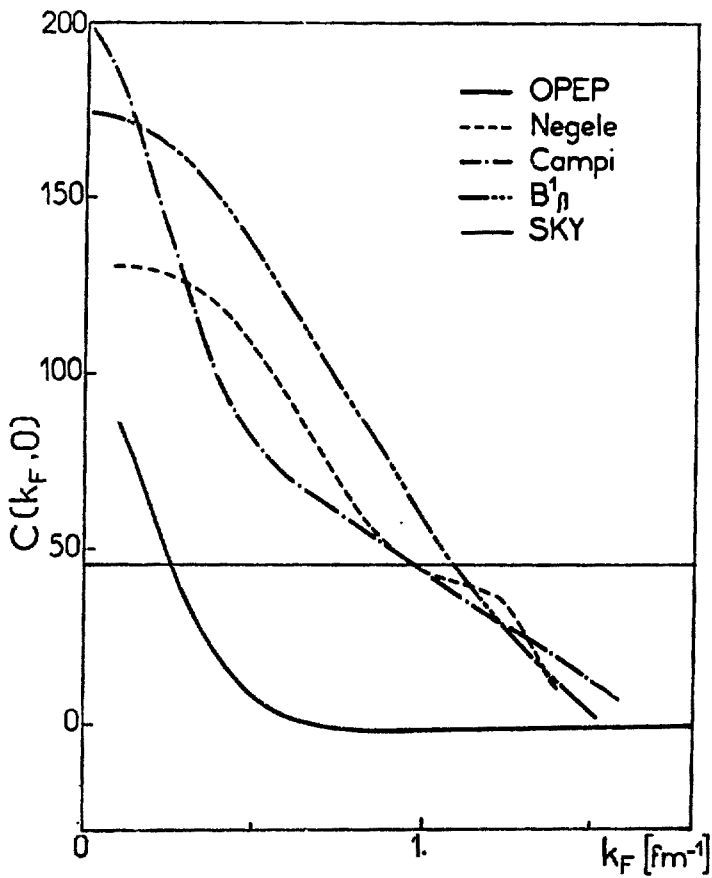


Fig. 4.

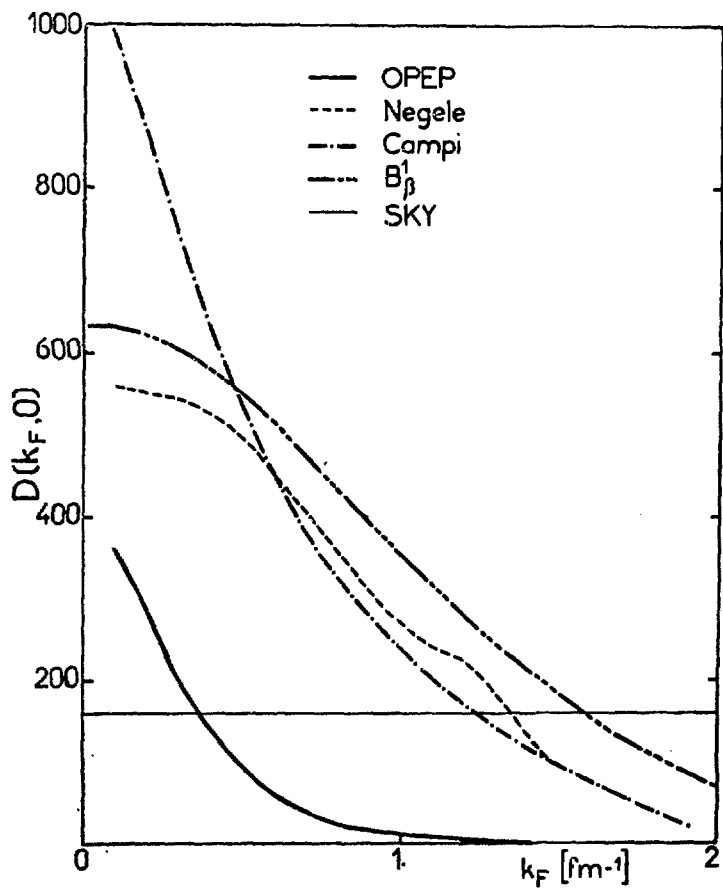


Fig. 5.

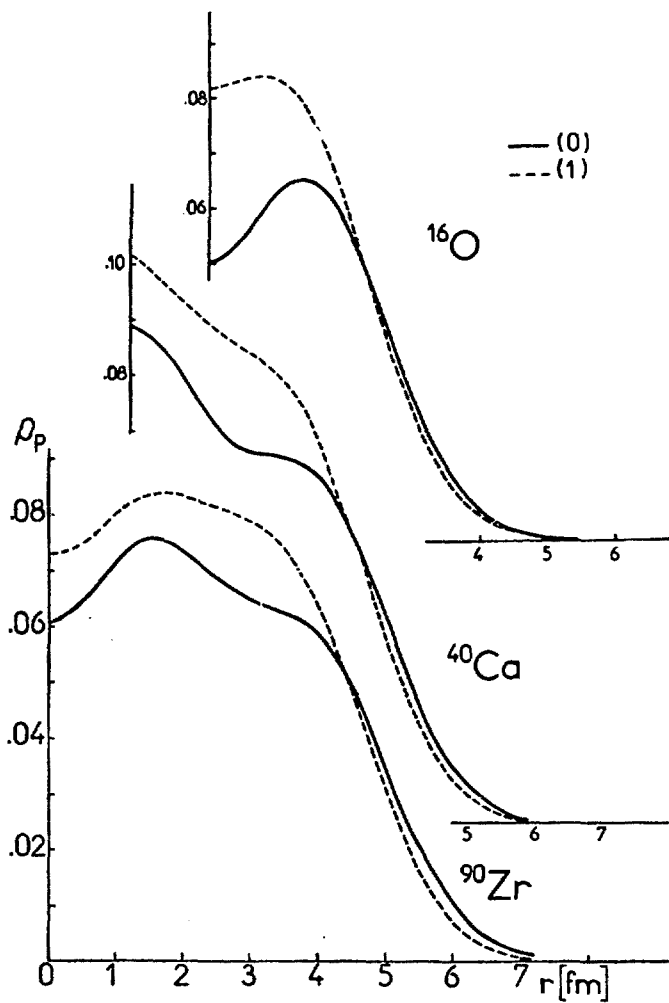


Fig. 6.

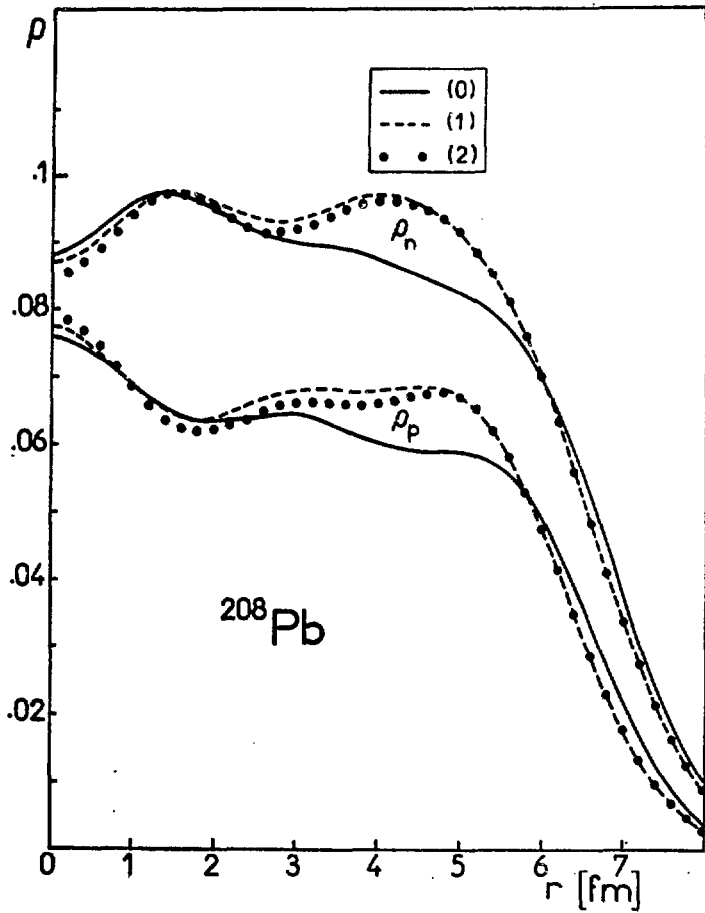


Fig. 7.

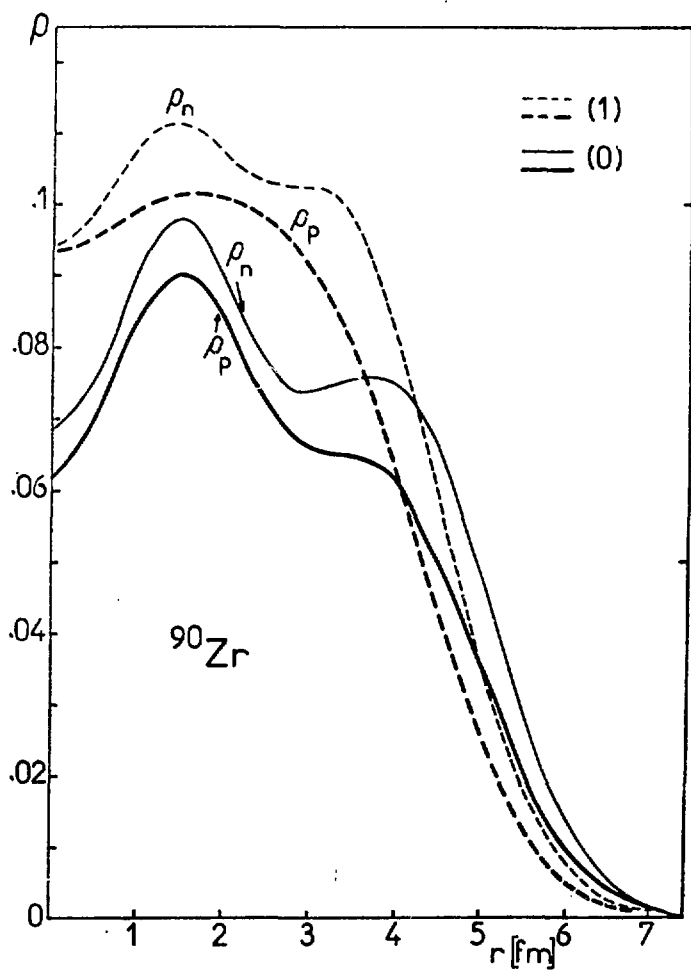


Fig. 8.

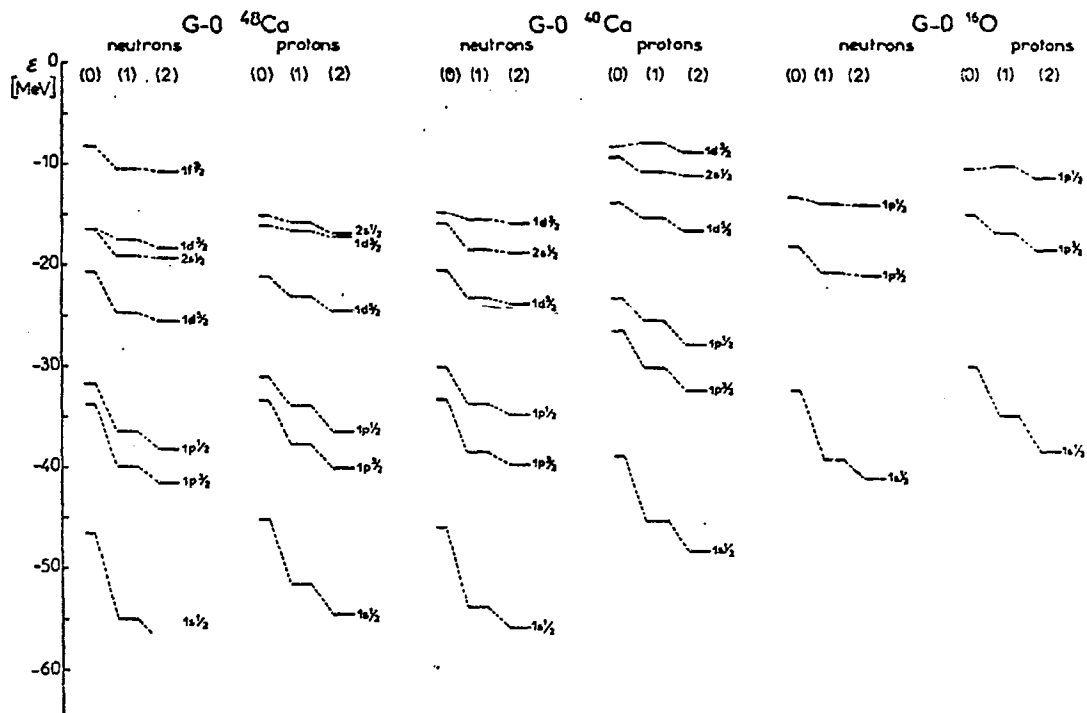


Fig. 9.

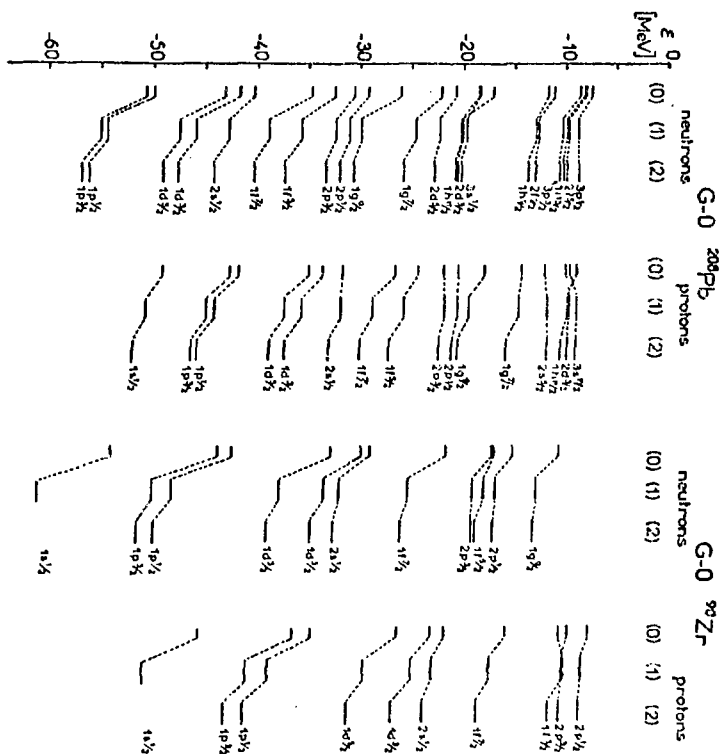


Fig. 10.

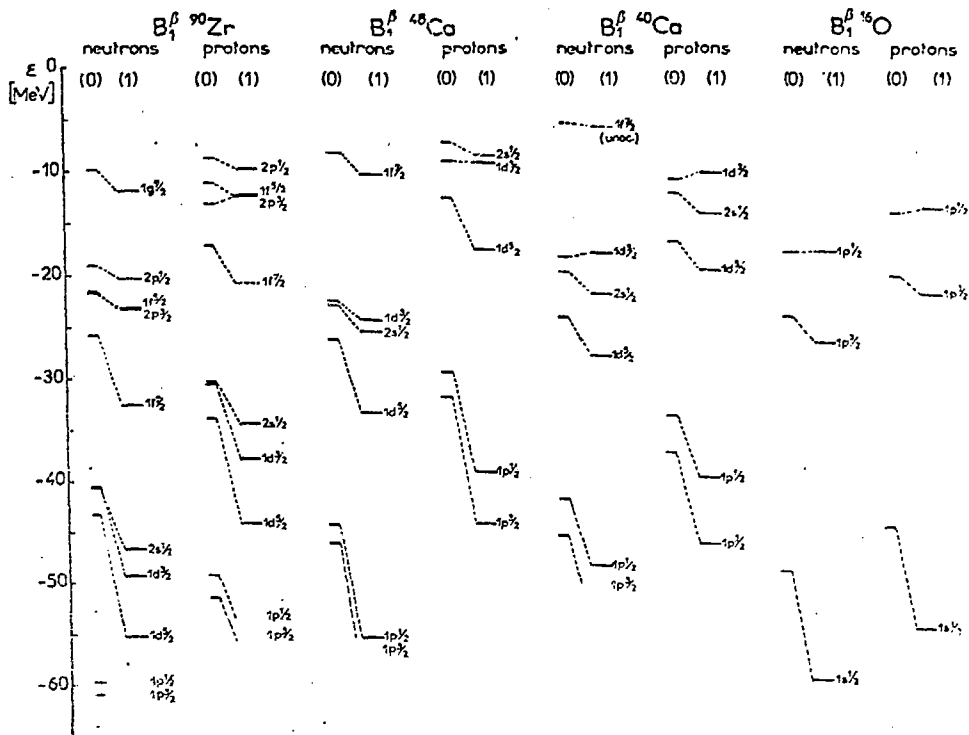


Fig. 11.

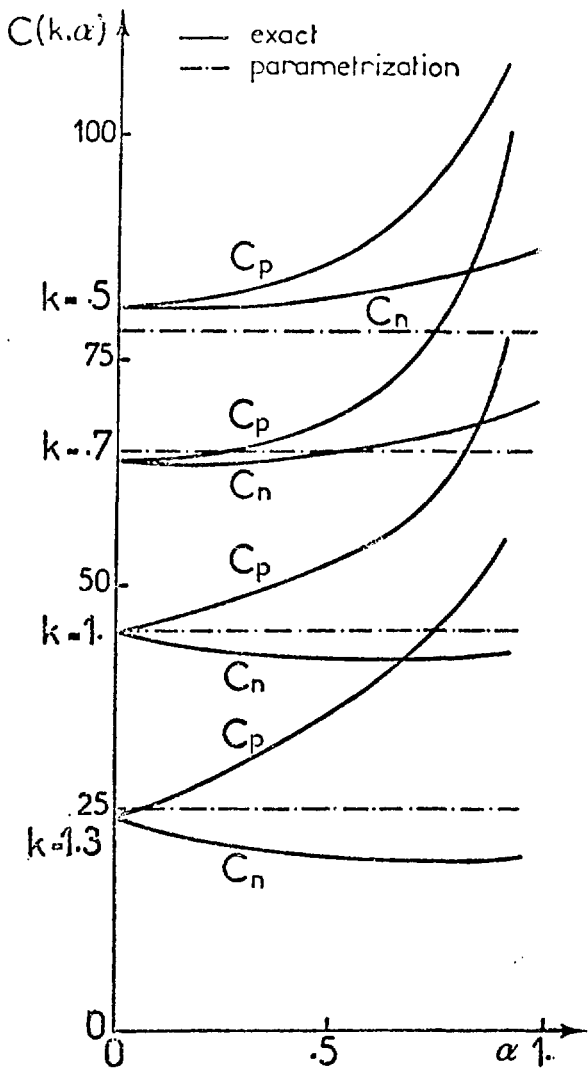


Fig. 12.

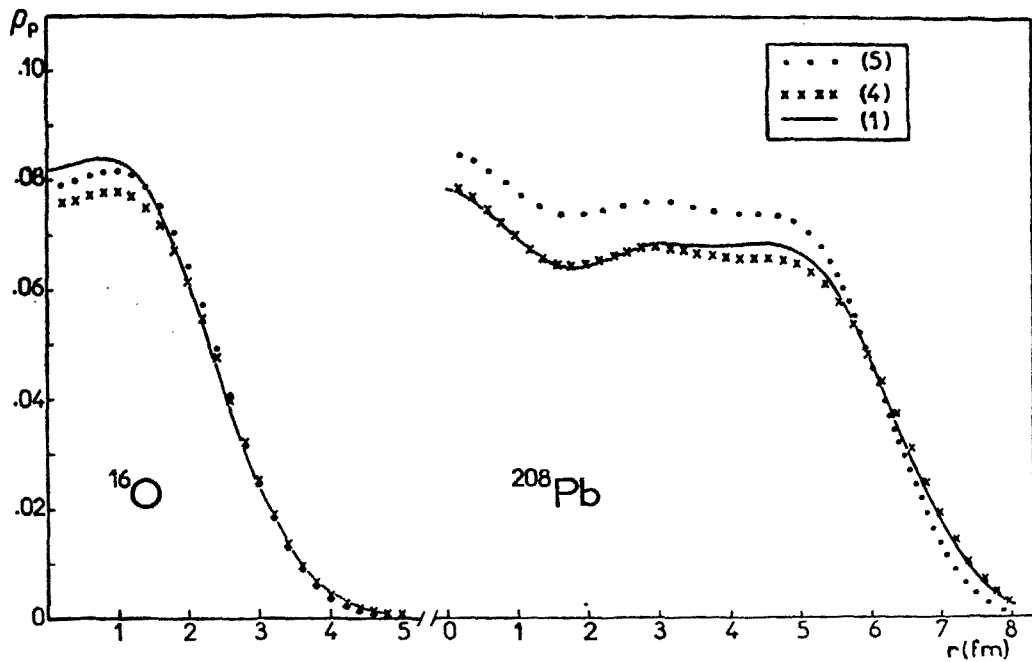


Fig. 13.

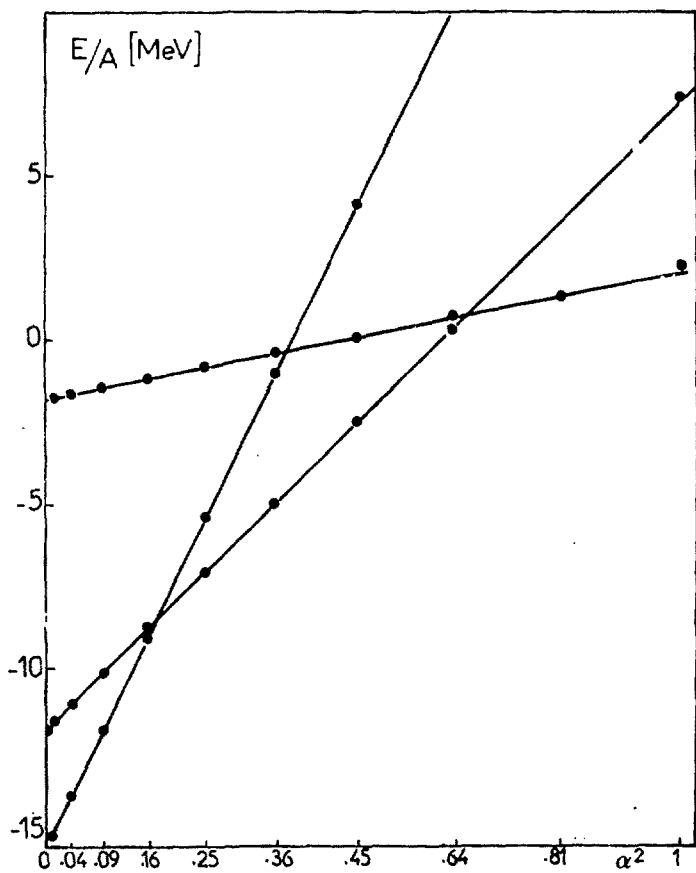


Fig. 14.

